Applied Radiation and Isotopes 120 (2017) 1–6

Contents lists available at ScienceDirect

Applied Radiation and Isotopes

journal homepage: www.elsevier.com/locate/apradiso

Assessing arsenic and selenium in a single nail clipping using portable X-ray fluorescence

David E.B. Fleming[a,*], Michel N. Nader[a], Kelly A. Foran[a], Craig Groskopf[a], Michael C. Reno[a], Chris S. Ware[a], Mina Tehrani[c], Diana Guimarães[b,c], Patrick J. Parsons[b,c]

[a] Physics Department, Mount Allison University, Sackville, NB, Canada
[b] Laboratory of Inorganic and Nuclear Chemistry, Wadsworth Center, New York State Department of Health, P.O. Box 509, Albany, NY 12201, USA
[c] Department of Environmental Health Sciences, School of Public Health, The University at Albany, P.O. Box 509, Albany, NY 12201, USA

ARTICLE INFO

Keywords:
Portable X-ray fluorescence
Arsenic
Selenium

ABSTRACT

The feasibility of measuring arsenic and selenium contents in a single nail clipping was investigated using a small-focus portable X-ray fluorescence (XRF) instrument with monochromatic excitation beams. Nail clipping phantoms supplemented with arsenic and selenium to produce materials with 0, 5, 10, 15, and 20 μg/g were used for calibration purposes. In total, 10 different clippings were analyzed at two different measurement positions. Energy spectra were fit with detection peaks for arsenic K_α, selenium K_α, arsenic K_β, selenium K_β, and bromine K_α characteristic X-rays. Data analysis was performed under two distinct conditions of fitting constraint. Calibration lines were established from the amplitude of each of the arsenic and selenium peaks as a function of the elemental contents in the clippings. The slopes of the four calibration lines were consistent between the two conditions of analysis. The calculated minimum detection limit (MDL) of the method, when considering the K_α peak only, ranged from 0.210 ± 0.002 μg/g selenium under one condition of analysis to 0.777 ± 0.009 μg/g selenium under another. Compared with previous portable XRF nail clipping studies, MDLs were substantially improved for both arsenic and selenium. The new measurement technique had the additional benefits of being short in duration (~3 min) and requiring only a single nail clipping. The mass of the individual clipping used did not appear to play a major role in signal strength, but positioning of the clipping is important.

1. Introduction

The use of human nail clippings as an indicator of exposure to certain trace elements has a number of advantages over alternative biomarkers such as hair, blood, or urine (He, 2011). Nail clippings are most commonly analyzed by inductively coupled plasma mass spectrometry (ICP-MS), following acid digestion, or by instrumental neutron activation analysis (INAA). One of the elements most often associated with nail clipping analysis is arsenic (Samanta et al., 2004; Slotnick et al., 2007). Recent work has explored the use of a portable X-ray fluorescence (XRF) approach to measuring arsenic in nail (Roy et al., 2010) or nail clippings (Gherase and Fleming, 2011). Compared with ICP-MS or INAA, the portable XRF technique is fast, simple to implement, applicable in the field, and cost effective. When considering arsenic determination in nail clippings, XRF can measure the selenium content at the same time and with similar sensitivity (Gherase and Fleming, 2011). This is potentially important because the metabolism of arsenic and selenium are interconnected (Gailer et al., 2000; Gailer, 2007). There is some evidence that the deleterious health effects resulting from exposure to arsenic may be mitigated by intake of selenium (Biswas et al., 1999; Gailer et al., 2000).

Portable XRF methods for nail clipping analysis explored to this point have demonstrated a strong dependence of signal strength and measurement sensitivity on the sample mass. This effect has been documented in a variety of calibration trials using artificial nail clippings (or "phantoms") analyzed for arsenic and selenium (Gherase and Fleming, 2011), manganese and zinc (Fleming et al., 2013), and (to a lesser extent) chromium (Fleming and Ware, 2016). As a result, nail clipping samples of low mass can be difficult to use in practice, potentially limiting both the measurement precision and the number of subjects able to be assessed from a given population. For example, a recent portable XRF study of arsenic in nail clippings from a human population recommended that, in the future, the clippings sample obtained from each individual subject should be at least 30 mg in mass (McIver et al., 2015).

The mass dependence observed in previous studies using portable

* Corresponding author.
E-mail address: dfleming@mta.ca (D.E.B. Fleming).

http://dx.doi.org/10.1016/j.apradiso.2016.11.015
Received 22 August 2016; Received in revised form 11 November 2016; Accepted 16 November 2016
Available online 19 November 2016

XRF with nail clippings is mainly attributable to the fairly large X-ray beam size used in the measurement. Portable XRF systems have typically shown effective beam diameters of about 7 mm (Gherase et al., 2010) or even slightly larger (Fleming and Ware, 2016). This requires many individual nail clippings, and therefore a relatively high total sample mass, in order to fully encompass the beam area. In the current study, we investigate for the first time the measurement of arsenic and selenium in nail clipping phantoms using a portable XRF system with a novel small-focus, monochromatic X-ray beam.

The XRF system used in this study was the HD Mobile (X-ray Optical Systems; East Greenbush, NY). The HD Mobile unit incorporates Doubly Curved Crystal (DCC) optics, providing a high intensity beam delivery to a spot size of only 1 mm diameter (Guimarães et al., 2016). This beam size is sufficiently small as to be entirely encompassed by the dimensions of a single nail clipping. This unique feature removes the requirement for multiple clippings within a single sample. The other key distinguishing feature of the HD Mobile approach is the ability to provide multiple monochromatic X-ray beams. In this particular application, the nearly mono-energetic beam of 17.4 keV (molybdenum K_α) was a very good match for the excitation of both arsenic (K-edge of 11.9 keV) and selenium (K-edge of 12.7 keV). The HD Mobile system itself is fully portable, and can be operated in either a handheld mode or as an integrated unit within its carrying case (Guimarães et al., 2016). All measurements described in the current paper were performed in the case mode.

2. Methods

The samples analyzed in this study consisted of phantom nail clippings supplemented with various amounts of arsenic and selenium. The method for phantom production has been described in detail previously (Gherase and Fleming, 2011; Roy et al., 2010). Briefly, phantom nails were produced from a commercial resin, salt (NaCl), and quantities of arsenic and selenium added from standard solutions. The phantom nails were prepared to a thickness of ~0.7 mm, with this value being selected to approximate the lower end of a range of human toenail thicknesses found by Johnson and Shuster (1994). The same concentrations of arsenic and selenium were chosen for a given phantom calibration sample, and resulted in a final mass fraction of: 0 μg/g; 5 μg/g; 10 μg/g; 15 μg/g; and 20 μg/g. Commercial nail clippers were used to create phantom nail clippings of various shapes and sizes from the prepared calibration material. The dimensions of a typical clipping were about 10 mm in length and 2 mm in width, although there were some irregularities in shape and variations in dimension between the different clippings. Two clippings of each concentration were used in this study. Since the phantom clippings were designed to resemble human nail clippings, they were not of identical mass. Each individual clipping was weighed; the clipping masses and the labeling scheme are provided in Table 1.

Using the HD Mobile system, each individual clipping was analyzed twice, once on two different positions. As an example, the labeled positions and placement for the two measurements of the 0 μg/g clipping #1 is shown in Fig. 1. As described by Guimarães et al. (2016), the HD Mobile system was operated under the "quantifying" setting, with a plastic matrix selected as the mode most suitable for the analysis (McIntosh et al., 2015). The measurement time was fixed at approximately 3 min (Guimarães et al., 2016). Following each measurement, the energy spectrum (number of counts as a function of energy bin) was downloaded, and transferred to Origin 9.1 software (OriginLab Co.; Northampton, MA) for subsequent analysis. The spectrum output was provided in 2048 different energy bins, increasing by increments of 0.016859 keV, with standards used to provide the initial energy calibration.

Table 1
Phantom nail clippings used in study, with individual clipping masses.

As (and Se) content (μg/g)	Clipping number	Clipping mass (mg)
0	1	18.3
	2	13.7
5	1	12.6
	2	18.4
10	1	20.7
	2	15.6
15	1	10.5
	2	10.5
20	1	19.7
	2	14.8

Energy spectra were analyzed over the range of 10–13 keV, using a series of Gaussian functions combined with a linear background. Each Gaussian function was centered on a different energy of detection, resulting from a particular element. In total, two energy peaks (K_α and K_β) were fit from arsenic, two peaks (K_α and K_β) from selenium, and one peak (K_α) from bromine (which was a natural constituent of the resin). The resulting equation of fit to provide the number of counts detected, f(x), was therefore fairly detailed, involving a total of 17 different parameters:

$$f(x)=P1e^{-P2(x-P3)^2}+\ P4e^{-P5(x-P6)^2}+P7e^{-P8(x-P9)^2}+\ P10e^{-P11(x-P12)^2}+P13e^{-P14(x-P15)^2}+P16x+P17$$

Here, the independent variable, x, is the energy (in keV), P_1 is the Gaussian peak amplitude for arsenic K_α, P_2 is an inverse peak width parameter for arsenic K_α, P_3 is the peak center for arsenic K_α, P_4 is the Gaussian peak amplitude for selenium K_α, P_5 is an inverse peak width parameter for selenium K_α, P_6 is the peak center for selenium K_α, P_7 is the Gaussian peak amplitude for arsenic K_β, P_8 is an inverse peak width parameter for arsenic K_β, P_9 is the peak center for arsenic K_β, P_{10} is the Gaussian peak amplitude for bromine K_α, P_{11} is an inverse peak width parameter for bromine K_α, P_{12} is the peak center for bromine K_α, P_{13} is the Gaussian peak amplitude for selenium K_β, P_{14} is an inverse peak width parameter for selenium K_β, P_{15} is the peak center for selenium K_β, P_{16} is the slope of a linear background, and P_{17} is the intercept of a linear background. For each measurement trial, values for all of the parameters noted above were recorded, along with their standard errors. The starting parameters for the peak centers noted above corresponded to the energy of the associated characteristic X-ray. P_3 was therefore initially set to 10.5 keV, P_6 to 11.2 keV, P_9 to 11.7 keV, P_{12} to 11.9 keV, and P_{15} to 12.5 keV. The peak centers were allowed to float by up to 0.1 keV in either direction in order to optimize the fit. There was considerable overlap between the arsenic K_β characteristic X-ray (11.7 keV) and the bromine K_α characteristic X-ray (11.9 keV), making the two energy peaks difficult to separate.

As part of the method design, the question of whether the fitting results would be dependent on different operators or operator approaches to the data analysis was addressed. For this reason, for all of the spectral data obtained, analysis was divided into two separate conditions and the analysis was performed twice. For the first condition, one operator was assigned to the data analysis, and this operator constrained all of the peak amplitudes in the fittings to require a positive (or zero) result. For the second condition, four different operators were assigned to the data analysis, with each operator analyzing five of the clippings (one of each concentration) at one position. These operators allowed the peak amplitudes to take on any value, positive, negative, or zero. The first condition may appear more logical since a negative contribution from a particular element in a sample is not physically possible. The second approach, however, is more correct in a statistical sense since a sample containing a zero concentration of a particular element should be equally likely to return a negative result as a positive result. Allowing for this possibility eliminates any bias toward an artificially high positive outcome in cases where the true concentration is zero (or very close to zero). This

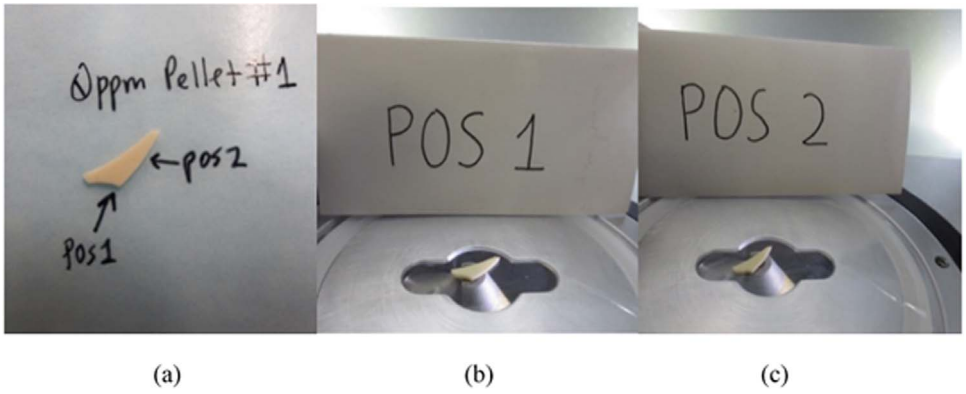

Fig. 1. (a) The two different measurement positions for the 0 μg/g clipping # 1. (b) The position 1 placement of the clipping on the window of the HD Mobile system. (c) The position 2 placement of the clipping on the window of the HD Mobile system.

approach has received considerable attention in the application of X-ray spectrometry to the measurement of lead in bone (Hoppin et al., 1995).

For both of the analysis conditions, the amplitude of the peak was examined from the arsenic K_α, selenium K_α, arsenic K_β, and selenium K_β characteristic X-rays for all of the various clipping trials. (The bromine K_α peaks were not considered in this portion of the exercise.) Each of the four detection peaks of interest were noted from the 10 clippings and with two different positions for each clipping. This resulted in a total of 80 different peak amplitude pairs to compare between the two analysis conditions. For a particular analysis condition and peak, the average peak height obtained from a given concentration of clipping was then considered as a function of concentration to determine a calibration line for the method. Individual calibration lines were determined for each peak, and under both of the analysis conditions. Finally, minimum detection limits (MDLs) in μg/g were calculated for the single nail clipping XRF method, based on the following formula: $MDL = \frac{3\sigma_0}{m}$

where σ_0 is the standard deviation of the peak amplitude in counts from the 0 μg/g clipping measurements, and m is the calibration line slope in counts per μg/g (Gherase et al., 2010). This general approach to calculating MDL is traditionally adopted for trace element detection in tissue using XRF (Da Silva et al., 2008; Studinski et al., 2006), and is also used here for ease of reference. It should be noted, however, that alternative approaches could be used (Kadachi and Al-Eshaikh, 2012).

3. Results

A typical energy spectrum resulting from the HD Mobile system when analyzing a clipping sample with arsenic and selenium concentrations of 20 μg/g is provided in Fig. 2, over the energy range of 10–20 keV. This view of the spectrum is dominated by the energy peak resulting from the Compton scatter of molybdenum K_α characteristic X-rays which arise from the X-ray tube and DCC optics configuration. Fig. 3 provides the same spectrum, but limited to the energy range of 10–13 keV. Here, the arsenic K_α (10.5 keV) and selenium K_α (11.2 keV) peaks are obvious and relatively large in amplitude. It is also evident that the overlap of the arsenic K_β (11.7 keV) and bromine K_α (11.9 keV) peaks makes it nearly impossible to distinguish these two different contributions by the naked eye. The selenium K_β (12.5 keV) peak is clear, although of relatively small amplitude, even when measuring this high concentration clipping. In this particular example, under the first condition of analysis, the amplitude returned for the arsenic K_α peak is 418 ± 8 counts, for the selenium K_α peak is 460 ± 9, for the arsenic K_β peak is 76 ± 142, for the bromine K_α peak is 199 ± 137, and for the selenium K_β peak is 66 ± 4. For each peak, the uncertainty provided is the standard error returned from the fitting procedure.

The difference in peak amplitude results from the two different analysis starting conditions were found to be mostly non-existent for some of the peaks, but significant for others. Overall, of the 80 pairs of peak amplitude results determined, 56 returned results within 5% of each other. Notably, this included all 16 of the 5 μg/g, 10 μg/g, 15 μg/

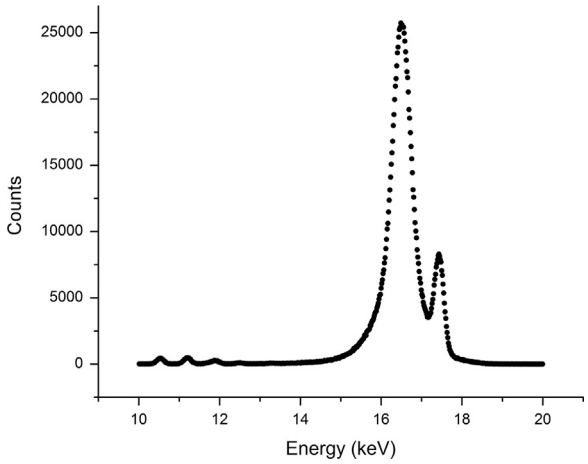

Fig. 2. The number of counts as a function of energy from the measurement of the 20 μg/g clipping # 2 at position 2. This view highlights the detection of the Compton scatter peak at ~16.5 keV which results from the Mo K_α characteristic X-rays produced by the X-ray tube and DCC optics configuation.

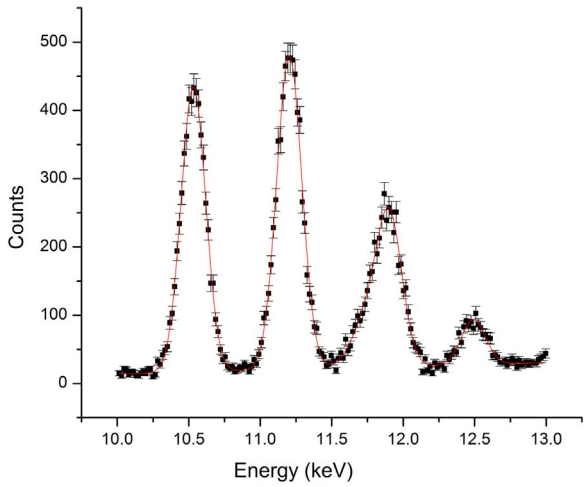

Fig. 3. The number of counts as a function of energy from the measurement of the 20 μg/g clipping # 2 at position 2. The uncertainty bars here represent the sqaure root of the number of counts. The continuous line represents the best fit of the function described in the main text, under the first condition of analysis. Characteristic X-rays are emitted at 10.5 keV (As K_α), 11.2 keV (Se K_α), 11.7 keV (As K_β), 11.9 keV (Br K_α), and 12.5 keV (Se K_β).

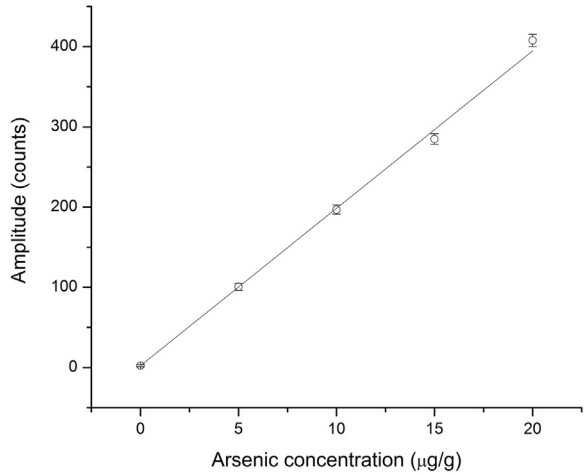

Fig. 4. Calibration line from the arsenic K_α peak measurements, under the first condition of analysis. The plot shows amplitude of the arsenic K_α peak as a function of arsenic content in the clipping. Each data point represents the average of four measurements (two different clippings at two different positions). The uncertainty bars here represent the average uncertainty from each point.

g, and 20 μg/g results obtained for the arsenic K_α peak, and all 16 of the 5 μg/g, 10 μg/g, 15 μg/g, and 20 μg/g results obtained for the selenium K_α peak. These pairs of results were all essentially identical to each other, with no single difference in amplitude exceeding 0.13%. The average of the absolute difference between the pairs of these amplitudes was only 0.02 counts. In addition, 15 of the 16 results from the 5 μg/g, 10 μg/g, 15 μg/g, and 20 μg/g selenium K_β peaks were within 5% of each other. However, only 9 of the 16 results from the 5 μg/g, 10 μg/g, 15 μg/g, and 20 μg/g arsenic K_β peaks were within 5% of each other. Furthermore, *all* of the 0 μg/g peak amplitude results from arsenic K_α, selenium K_α, arsenic K_β, and selenium K_β differed by more than 5%. The average of the absolute difference between the pairs of amplitudes obtained from the 0 μg/g measurements was 3.2 counts.

Calibration lines were created for each of the four peaks of interest and under both analysis conditions, as described above. This resulted in a total of eight calibration lines. As examples, Fig. 4 presents the calibration line from the arsenic K_α measurements under the first condition (not allowing the possibility of a negative amplitude result), while Fig. 5 provides the calibration line from the selenium K_α

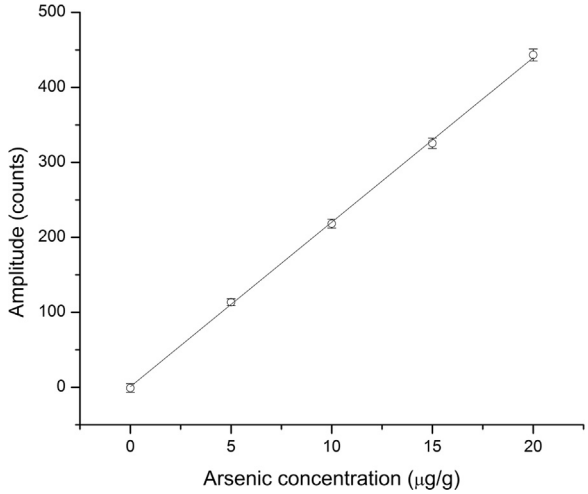

Fig. 5. Calibration line from the selenium K_α peak measurements, under the first condition of analysis. The plot shows amplitude of the selenium K_α peak as a function of selenium content in the clipping. Each data point represents the average of four measurements (two different clippings at two different positions). The uncertainty bars here represent the average uncertainty from each point.

Table 2
Parameters from the linear equations of best fit for calibration lines resulting from the four peaks of interest and two conditions of analysis.

Peak analyzed and condition of analysis		Slope (g/μg)	Intercept	r^2
As K_α;	1st condition	19.5 ± 0.4	3 ± 3	0.9982
	2nd condition	19.6 ± 0.4	2 ± 2	0.9985
Se K_α;	1st condition	21.9 ± 0.2	1 ± 1	0.9998
	2nd condition	21.9 ± 0.3	1 ± 3	0.9994
As K_β;	1st condition	3.1 ± 0.7	7 ± 8	0.8168
	2nd condition	2.9 ± 0.4	5 ± 5	0.9105
Se K_β;	1st condition	2.8 ± 0.2	2 ± 2	0.9858
	2nd condition	3.0 ± 0.1	−1 ± 2	0.9905

Table 3
Minimum detection limits resulting from the four peaks of interest and two conditions of analysis.

Peak analyzed and condition of analysis		Minimum detection limit (μg/g)
As K_α;	1st condition	0.293 ± 0.006
	2nd condition	0.223 ± 0.004
Se K_α;	1st condition	0.210 ± 0.002
	2nd condition	0.777 ± 0.009
As K_β;	1st condition	80 ± 20
	2nd condition	90 ± 10
Se K_β;	1st condition	2.9 ± 0.2
	2nd condition	2.3 ± 0.1

measurements under the first condition. A presentation of the slopes and intercepts from the various calibration lines under the two conditions of analysis is provided in Table 2. Finally, the MDLs determined individually from each of the four detection peaks of interest, and under both conditions of analysis, are provided in Table 3.

4. Discussion

Over the region of interest, from 10 to 13 keV in the current study, the energy spectra from the HD Mobile system returned low background contributions. The energy spectrum shown in Fig. 3 was typical, with the background ranging in size from about 14 counts near 10 keV to about 30 counts near 13 keV. The low background over this region was a consequence of the mono-energetic nature of the source (17.4 keV): in order to result in a background detection between the energies 10–13 keV, a photon with an initial energy of 17.4 keV would need to undergo a low probability combination of multiple scattering events. This low background facilitated analysis of the elemental signals, especially in the case of the lower energy peaks from arsenic K_α (10.5 keV) and selenium K_α (11.2 keV). Relative to more conventional portable XRF systems, the HD Mobile also presented an intense beam of photons relatively close to the K-edges of both arsenic and selenium. This resulted in an efficient excitation of characteristic X-rays from arsenic and selenium.

For a given calibration phantom, there did not appear to be a direct relationship between the arsenic or selenium signal and the mass of the clipping. For example, for the 10 μg/g clippings, the higher mass clipping # 1 (20.7 mg) provided on average slightly lower arsenic and selenium amplitudes than the lower mass clipping # 2 (15.6 mg). From visual inspection of the clipping images and positions, however, it did appear that higher signals might be associated with the width of the clipping at the position of measurement. It is also possible that slight variations in clipping thickness could influence measurement results. These factors would be especially important to consider if measuring real human nail clippings, where variations would be more pronounced. In addition, curvature of the clipping could become a factor with real nail clippings, as could inhomogeneity in elemental distribution (Gherase et al., 2013). While beyond the scope of the current study, it is recommended that a careful investigation of these factors and the

positioning of the clipping sample be pursued in future studies.

As part of the study design, the question of whether changing conditions of analysis would influence results was addressed. Specifically, two separate analysis conditions were investigated: the first condition constrained the fitting to return a positive (or zero) peak amplitude in all cases; the second condition also permitted negative peak amplitudes. While the fitting of energy spectra was robust and unaffected by our conditions of analysis for the arsenic K_α and selenium K_α clipping concentrations of 5 μg/g, 10 μg/g, 15 μg/g, and 20 μg/g, there were two observed categories of analysis which were affected by the analysis condition. The fitting of the arsenic K_β peak (11.7 keV), which was entangled with the nearby bromine K_α peak (11.9 kev), was often found to be influenced by choice of analysis condition. Additionally, the results were always at least somewhat dependent on condition of analysis when the 0 μg/g clippings were analyzed. (This was not surprising given that the first condition eliminated the possibility of a negative amplitude value.) The latter category was more concerning since it influenced all four of the peak measurements. However, while the relative differences between analysis condition pairs of results were always greater than 5% in this category, the absolute differences were not especially large (3.2 counts on average). A difference of 3.2 counts converts to about 0.16 μg/g when analyzing the arsenic K_α peak, and about 0.15 μg/g when analyzing the selenium K_α peak. There was no apparent effect on the results related to the four different operators carrying out the data analysis under the second condition. For example, all four of these operators returned results nearly identical to those from the first condition of analysis for the arsenic K_α and selenium K_α clipping concentrations of 5 μg/g, 10 μg/g, 15 μg/g, and 20 μg/g. Where significant differences did emerge, they appeared to relate entirely to the condition of analysis, as described above.

Interestingly, these differences in the fitting of results from individual clipping samples based on condition of analysis did not translate into significant differences between the calibration lines. As demonstrated by Table 2, the linear equation of best fit was very similar between the two conditions of analysis in every instance. In general, the first condition of analysis tended to result in a slightly higher intercept term. This finding was expected, given that the first condition of analysis was constrained to return a positive (or zero) amplitude for each peak, while the second condition was not. Overall, the coefficients of determination (r^2) were very high for all of the calibration lines, with the exception of the arsenic K_β lines. The slope of the calibration lines were slightly larger from the selenium K_α peak results compared to those determined from the arsenic K_α results. The reason for this was twofold. First of all, the mono-energetic beam energy (17.4 keV) of the HD Mobile system was closer to the K-edge of selenium, resulting in a slightly more efficient excitation of selenium K X-rays. Secondly, the higher energy of the selenium K_α characteristic X-rays (11.2 keV) resulted in less attenuation of these photons, relative to the arsenic K_α X-rays (10.5 keV). For both arsenic and selenium, the K_α slopes were, of course, much larger than the corresponding K_β slopes. The observed K_α:K_β slope ratios ranged from 6.3 ± 1.4 to 7.8 ± 0.6, consistent with the expected ratios of ~7.6 (Kortright and Thompson, 2001). (This expected value assumes full detection of the $K_{\alpha1}$ and $K_{\alpha2}$ X-rays in the K_α peak, full detection of the $K_{\beta1}$, $K_{\beta2}$, and $K_{\beta3}$ X-rays in the K_β peak, and no differences in photon attenuation based on energy.) It is notable that even with the considerable interference of the arsenic K_β peak introduced by the bromine in the clipping samples, the slope values from the arsenic K_β results were consistent with those from the selenium K_β, albeit with larger uncertainties.

The minimum detection limits (MDLs) determined from the present study of single nail clipping phantoms indicate typical values of approximately ≤ 0.3 μg/g for both arsenic and selenium, based only on the K_α peak detections. The calculation of MDL used here is susceptible to fluctuations in the σ_0 parameter. Variations in σ_0 can be substantial in situations with a small number of trials, and this is likely the explanation for the unusually large MDL value of ~0.8 μg/g calculated from the selenium K_α peak under the second analysis condition. Additionally, relative variations in σ_0 can be large even when the absolute differences are quite small. Detection limits could be improved by making use of both the K_α and K_β detections from a given element. In the case of arsenic, this approach is not worthwhile for the current samples, given the very low precision of the K_β measurement. For selenium, however, the additional use of the K_β peak results in a modest improvement of about 5% in MDL for the second analysis condition. In any case, a detection limit of ≤ 0.3 μg/g from a single nail clipping is a considerable improvement over previous portable XRF work. Using a different portable XRF system with an effective beam diameter of about 7 mm (but using the same definition of MDL), calibration trials indicated that a 20 mg clipping mass resulted in an MDL of ~2 μg/g for both arsenic and selenium (Gherase and Fleming, 2011). Additionally, this previous method required a total sample irradiation time of 15 min, five times longer than in the current study.

Real human nail clippings will contain levels of arsenic and selenium which reflect exposure. External contamination of clippings is a possibility, but a number of washing procedures have been developed to reduce or eliminate any external contribution (Slotnick and Nriagu, 2006). Studies of arsenic and selenium in human nail clippings suggest levels which are greater than or similar to the MDL demonstrated in the current study. For example, recent ICP-MS analyses from a Canadian population showed mean fingernail arsenic results of 0.4 μg/g in unexposed individuals, and 0.9 μg/g in individuals exposed through moderately elevated concentrations of arsenic in drinking water (McIver et al., 2015). A study of clippings from British men using INAA found a geometric mean fingernail selenium result of 0.6 μg/g (Allen et al., 2004).

In summary, the introduction of a DCC optic-enabled system as a portable XRF approach to determining arsenic and selenium in nail clippings offers a number of potential advancements over other portable XRF methods. Sensitivity of measurement is much improved, even with a reduced time of measurement. The dependence of signal upon sample mass is reduced, although further consideration should be given to questions of clipping placement and clipping dimensions. The HD Mobile instrument appears to be capable of determining arsenic and selenium from a single nail clipping, provided the elemental mass fraction is moderately high (~0.3 μg/g). A potential disadvantage of this small-beam technique is that it makes individual measurements more susceptible to elemental inhomogeneity across a single clipping. Consideration should therefore be given to making multiple measurements across a clipping in order to assess an average result.

Acknowledgements

This work was supported by a Discovery Grant from the Natural Sciences and Engineering Research Council of Canada. We acknowledge the assistance of Elstan Desouza in helping to establish this collaborative study.

References

Allen, N.E., Morris, J.S., Ngwenyama, R.A., Key, T.J., 2004. A case-control study of selenium in nails and prostate cancer risk in British men. Br. J. Cancer 90, 1392–1396.

Biswas, S., Talukder, G., Sharma, A., 1999. Prevention of cytotoxic effects of arsenic by short-term dietary supplementation with selenium in mice in vivo. Mutat. Res. – Genet. Toxicol. Environ. Mutagen. 441, 155–160.

Da Silva, E., Pejović-Milić, A., Heyd, D.V., 2008. The use of teeth as the site for the in vivo or ex vivo quantification of skeletal strontium by energy-dispersive X-ray fluorescence spectrometry: a feasibility study. J. Anal. At. Spectrom. 23, 527–534.

Fleming, D.E.B., Ware, C.S., 2016. Portable X-ray fluorescence for the analysis of chromium in nail and nail clippings. Appl. Radiat. Isot., (under review).

Fleming, D.E.B., Gherase, M.R., Anthonisen, M., 2013. Calibrations for measurement of manganese and zinc in nail clippings using portable XRF. X-Ray Spectrom. 42, 299–302.

Gailer, J., 2007. Arsenic-selenium and mercury-selenium bonds in biology. Coord. Chem.

Rev. 251, 234–254.
Gailer, J., George, G.N., Pickering, I.J., Prince, R.C., Ringwald, S.C., Pemberton, J.E., Glass, R.S., Younis, H.S., DeYoung, D.W., Aposhian, H.V., 2000. A metabolic link between arsenite and selenite: the seleno-bis (S-glutathionyl) arsinium ion. J. Am. Chem. Soc. 122, 4637–4639.
Gherase, M.R., Fleming, D.E.B., 2011. A calibration method for proposed XRF measurements of arsenic and selenium in nail clippings. Phys. Med. Biol. 56, N215–N225.
Gherase, M.R., Mader, J.E., Fleming, D.E.B., 2010. The radiation dose from a proposed measurement of arsenic and selenium in human skin. Phys. Med. Biol. 55, 5499–5514.
Gherase, M.R., Desouza, E.D., Farquharson, M.J., McNeill, F.E., Kim, C.-Y., Fleming, D.E.B., 2013. X-ray fluorescence measurements of arsenic micro-distribution in human nail clippings using synchrotron radiation. Physiol. Meas. 34, 1163–1177.
Guimarães, D., Praamsma, M.L., Parsons, P.J., 2016. Evaluation of a new optic-enabled portable X-ray fluorescence spectrometry instrument for measuring toxic metals/metalloids in consumer goods and cultural products. Spectrochim. Acta Part B 122, 192–202.
He, K., 2011. Trace elements in nail as biomarkers in clinical research. Eur. J. Clin. Investig. 41, 98–102.
Hoppin, J.A., Aro, A.C.A., Williams, P.L., Hu, H., Ryan, P.B., 1995. Validation of K-XRF bone lead measurement in young adults. Environ. Health Perspect. 103, (78-73).
Johnson, M., Shuster, S., 1994. Determinants of nail thickness and length. Br. J. Dermatol. 130, 195–198.
Kadachi, A.N., Al-Eshaikh, M.A., 2012. Limits of detection in XRF spectroscopy. X-Ray Spectrom. 41, 350–354.
Kortright, J.B., Thompson, A.C., 2001. X-ray emission energies. In: X-ray Data Booklet, second edition, Lawrence Berkeley National Laboratory, Berkeley, CA, pp. 1-15–1-27
McIntosh, K.G., Guimarães, D., Cusak, M.J., Vershinin, A., Chen, Z.W., Yang, K., Parsons, P.J., 2015. Evaluation of portable XRF instrumentation for assessing potential environmental exposure to toxic elements. Int. J. Environ. Anal. Chem. 96, 15–37.
McIver, D.J., VanLeeuwen, J.A., Knafla, A.L., Campbell, J.A., Alexander, K.M., Gherase, M.R., Guernsey, J.R., Fleming, D.E.B., 2015. Evaluation of a novel portable X-ray fluorescence screening tool for detction of arsenic exposure. Physiol. Meas. 36, 2443–2459.
Roy, C.W., Gherase, M.R., Fleming, D.E.B., 2010. Simultaneous assessment of arsenic and selenium in human nail phantoms using a portable X-ray tube and a detector. Phys. Med. Biol. 55, N151–N159.
Samanta, G., Sharma, R., Roychowdhury, T., Chakraborti, D., 2004. Arsenic and other elements in hair, nails, and skin-scales of arsenic victims in West Bengal, India. Sci. Total Environ. 326, 33–47.
Slotnick, M.J., Nriagu, J.O., 2006. Validity of human nails as a biomarker of arsenic and selenium exposure: a review. Environ. Res. 102, 125–139.
Slotnick, M.J., Meliker, J.R., Ruskin, G.A., Ghosh, D., Nriagu, J.O., 2007. Toenails as a biomarker of inorganic arsenic intake from drinking water and foods. J. Toxicol. Environ. Health Part A 70, 148–158.
Studinski, R.C.N., McNeill, F.E., O'Meara, J.M., Chettle, D.R., 2006. A method detection limit for potential in vivo arsenic measurements with a 50 W X-ray tube. Phys. Med. Biol. 51, N381–N387.